Optical Scattering as a Probe of Local Field Effect in Micron-sized CdS Spheres

Seong Kyu Kim*, Alan L. Huston‡, and Anthony J. Campillo‡

**Department of Chemistry, Sung Kyun Kwan University, Suwon 440-746, Korea*
‡Naval Research Laboratory, Washington, D.C. 20375-5338, U. S. A.
Received September 1, 1994

The optical properties of individual 3- to 14-micron diameter CdS crystalline spheres embedded in poly(methyl methacrylate) were studied using elastic scattering. The presence of well defined sharp peaks in the 550 to 600 nm elastic scattering spectra confirmed that each microcrystal acts as an optical cavity with cavity quality factors exceeding 10^4. Such natural resonator microcrystals should lead to greatly enhanced local field effects near the surface of CdS, quantum electrodynamic modification of optical transition rates of nearby species and altered photochemistry. Absorptive heating following high intensity laser irradiation was found to induce a transient washout of the high Q modes.

Introduction

Spherical microcrystals of various compounds (*e.g.* metal oxides and sulfides) may be prepared by homogeneous precipitation.[1] Microphotographs of these crystals show that they exhibit a highly symmetric morphology. It has been known for some time that when regulary shaped particles (spheres, spheroids and cylinders) become comparable in size to the wavelength of light, a significant local field effect occurs; *i.e.* optical fields near the crystal surface are enhanced many times that of the incident radiation's intensity.[2] This phenomena, for example, contributes to surface enhanced Raman scattering from metal surfaces and particles.[3] A similar enhancement in spontaneous Raman signal was observed from copper phthalocyanine deposited on nonmetallic GaP microcrystals.[4] In principle, chemically reacting fluorophors may be used to coat such microspheres to fabricate ultrasensitive optrodes for chemical species detection. Recently, Wang[5] noted that CdS, a commonly used photocatalyst, should exhibit strong local field enhancement (*ca.* 20 times). There has been a resurgence in interest in CdS microcrystals and colloids due to their unique photochemistry, their potential use in solar cells and as an electrophotographic material. Considering the impact of microcavity effects on photocatalytic colloid spectroscopy as well as directly on the specific details of their photochemistry, very little work has been reported in the literature. Wang[5] presented experimental data for a nearly monodisperse distribution of 1.1 μm diameter spherical CdS particles. His low temperature luminescence spectra showed several broad features that seemed to correlated with calculated spectra. It was suggested that the observed ripple structure was the result of cavity resonances. Because the experiments were performed on collection of particles of various sizes that often made contact with each other, the visual appearance of the spectral features may have been artificially broadened.

In this report we describe elastic scattering experiments on individual 3- to 14-micron diameter CdS spherical particles. We observe well-defined sharp peaks in the red wavelength elastic scattering spectra that indicate that these microcrystals are indeed behaving as high quality natural optical cavities. A lower bound on the cavity quality factor Q of 2×10^3 was confirmed from direct resonance width data. We discuss the implications of the presence of a high quality microcavity on the photophysics and photochemistry of these particles. We also observe that absorptive heating of the crystal following high intensity laser irradiation induces a transient washout of the high Q modes.

S. K. Kim dedicates this paper to Professor Woon-Sun Ahn on the occasion of his retirement.

Theory

Scattering of a plane wave of wavelength λ by a spherical particle of radius a and index m into polar angles θ and φ is calculated using the Lorenz-Mie formalism[6]. In practice, all fields both internal and external to the spheres are exactly calculable using digital computers. Here, m is the ratio of particle index of refraction to that of the surrounding space. Using the notation of Reference 6, the scattererd light intensity outside the sphere that is polarized in the φ and θ azimuths, respectively, is given by

$$I_\phi=\frac{\lambda}{4\pi^2r^2}\ |S_1|^2\ \sin^2\phi \tag{1}$$

$$I_\theta=\frac{\lambda}{4\pi^2r^2}\ |S_2|^2\ \cos^2\phi \tag{2}$$

where

$$S_1=\sum_{n=1}^{\infty}\frac{2n+1}{n(n+1)}\{a_n\pi_n(\cos\theta)+b_n\tau_n(\cos\theta)\}(-1)^{n+1} \tag{3}$$

$$S_2=\sum_{n=1}^{\infty}\frac{2n+1}{n(n+1)}\{a_n\tau_n(\cos\theta)+b_n\pi_n(\cos\theta)\}(-1)^{n+1} \tag{4}$$

a_n and b_n are scattering coefficients[6] that are formed from spherical Bessel functions of order n and with arguments $x(x=2a\pi/\lambda)$ or mx. π_n and τ_n are Legendre polynomial functions of the first kind of degree n and argument cosθ. When computing elastic scattering spectra, the variables entering the calculation include θ, λ, x and m. Our computational programs include a version[7] of a published routine for determining the values of the required spherical Bessel functions.

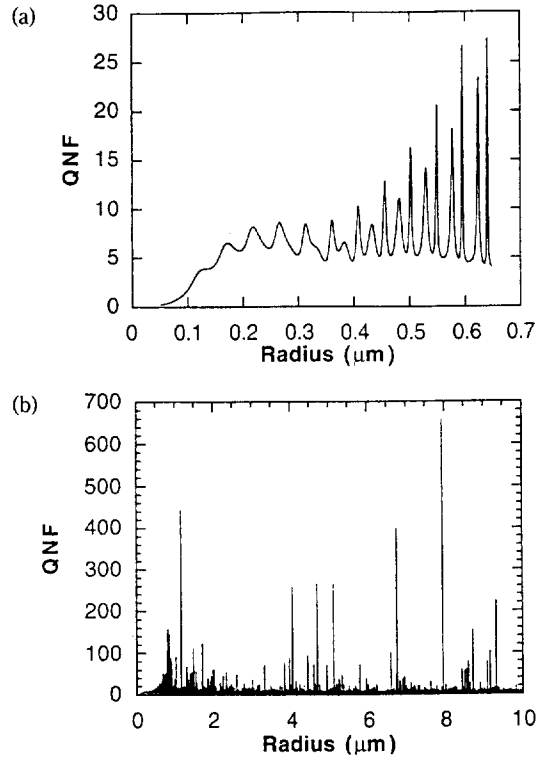

Figure 1. Q_{NF}, a measure of the local field enhancement, is plotted against particle radius. This quantity is calculated from Lorenz Mie theory by angle averaging field intensity over the particle surface. In the case shown, a CdS sphere (index 2.51) embedded in PMMA (index 1.45) at a wavelength of 641 nm is assumed. (a) shows the local field enhancement for particles up to 0.7 μm in size. The enhancement at very small size is dominated by particle lensing which tends to concentrate the light near the back surface (see Figure 2(a)). The sharp peaks occuring for radii greater than 0.4 μm result from the particle acting as a high Q cavity (see Figure 2(b)). (b) shows that local field enhancement for particles as large as 10 μm exceeds 600 when on resonance.

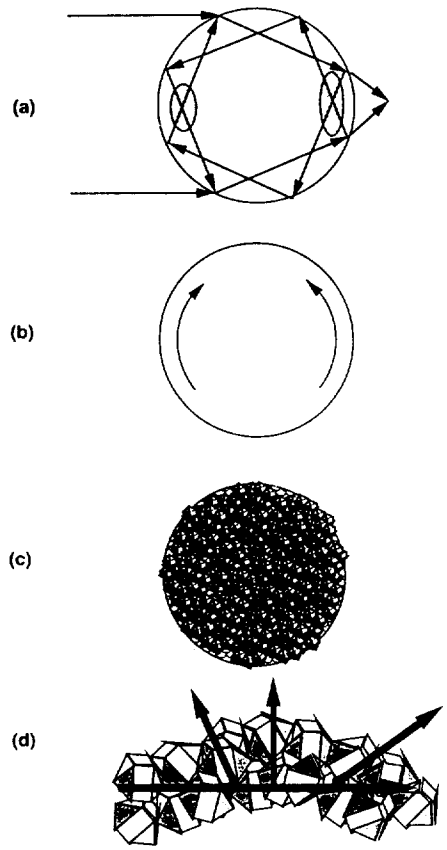

Figure 2. The origin of the local field enhancement and characteristic elastic scattering behavior is depicted in this Figure. (a) illustrates that a transparent microsphere forms a lens and concentrates incident light at the shadow side. Some of the rays shown are internally reflected and form another hot spot near the entrance face. These hot spots lead to an average surface electric field which is much greater than the incident value. (b) illustrates that the particle also acts a high Q optical cavity. Waves circulate near the surface by total internal reflection (here shown as two counterpropagating waves) and eventually fold back on themselves in phase when the circumference equals an integral number of wavelengths. Resonant enhancements are evident as sharp features in Figure 1(b). (c) depicts schematically that experimental CdS spheres are not homogeneous but are composed instead of tightly packed, randomly oriented, submicron, hexagonal and birefringent (n_e=2.511, n_o=2.493 at 600 nm) crystallites, Consequently, circulating resonant waves as in (b) experience strong multiple reflections and scattering as depicted in (d). These internally and surface scattered waves are the principal output coupling mechanism of these CdS cavities.

Calculations are performed on either a Macintosh II Personal Computer or a Cray XMP-24, depending on the desired spectral resolution.

Equations 1 to 4 allow the far field intensity to be calculated. Messinger *et al.*[2] introduced a parameter, Q_{NF}, which gives a measure of the angle averaged field intensity at the surface (*i.e.* local field effect) of the particle. This parameter is given by

$$Q_{NF}=2\sum_{n=1}^{\infty}\{|a_n|^2[(n+1)|h_{n-1}^{(2)}(x)|^2+n|h_{n-1}^{(2)}(x)|^2] + (2n+1)\ |b_n|^2|h_n^{(2)}(x)|^2\} \quad (5)$$

where $h_n^{(2)}$ is the Hankel function of the second kind. Using equation (5), index of refraction data[8] for CdS, and assuming the crystal is embedded in poly(methyl methacrylate) (PMMA), (refractive index=1.45), Q_{NF} was calculated at 641 nm as a function of crystal radius in Figure 1. Figure 1(a) shows that increasing particle radius from small values initially leads to an increase in Q_{NF} to a maximum value of 8-10 at 0.25 μm size. As the size is increased further, additional sharp peaks form and Q_{NF} approaches 30. Figure 1(b) shows a calculation of particles up to 10 μm in radius. Here peaks as high as 660 are observed sitting atop an enhancement plateau of 6 to 10. In this latter size range, the plateau is due to the spherical crystal acting as a lens (see Figure 2(a)). Rays are brought to a focus just beyond the shadow surface. These rays, which lead to "rainbow" phenomena in atmospheric water droplets, reflect several times internally and form high intensity regions at the input (100× en-

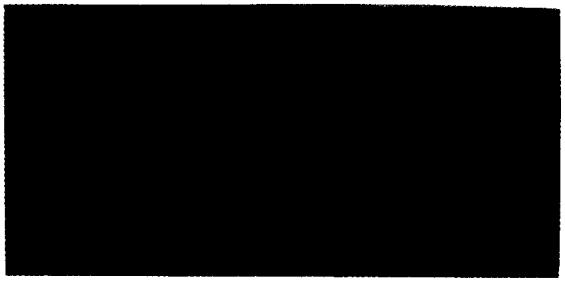

Figure 3. A highly magnified (1000×) photograph of an 8 micron diameter CdS sphere embeded in PMMA film.

hancement) and output (300×) faces near the equator.[9] The sharp peaks are very interesting and are due to the particle acting as an optical cavity[10,11]; feedback is provided by light waves that totally internally reflect at the interface and fold back on themselves (see Figure 2(b) showing two counter-propagating waves). Such resonances are designated by several mode numbers. The principal mode number, n, indicates the order of the spherical Bessel and Hankel functions describing the partial-wave radial field distribution and the order, l, indicates the number of maxima in the radial dependence of the internal field distribution. Both transverse electric, TE, and transverse magnetic, TM, resonances exist. Such resonances are often called morphology dependent resonances (MDR's).[11,12] The quality factors, Q, of these resonances may be determined from the spectral width ($Q=\lambda/\Delta\lambda=x/\Delta x$) of calculated or observed elastic scattering spectra. The Q factors vary with l number, the highest Q modes being the $l=1$ modes. These have been experimentally measured to be as high as 10^8 in liquid droplets.[13] Resonant modes lie spatially near the surface of the particle and cause light fields to build to very high value.[10] It was shown[14] from asymptotic relationships that the ratio of the intensity of the circulating resonant wave to that of the incident wave is given by the ratio $3Qm/x^2$. In principle, a particle of size parameter $x=75$ having a Q of 10^8 will exhibit an enhancement of *ca.* 10^5. In an effort to determine the maximum value of Q in CdS spheres we conducted elastic scattering experiments.

Experimental Section

CdS spheres were grown from aqueous solution using a two-step procedure.[1,5] The first step involved the growth of "seed" crystals of approximately 0.1 micron radius by aging a solution of 0.0012 M $Cd(NO_3)_2$, 0.24 M HNO_3 and 0.0050 M thioacetamide for approximately 15 hours. Larger particles were then grown by adding 6 mL of 0.050 M thioacetamide to a 500 mL volume of the seed solution and allowing the growth process to proceed for one hour. The majority of the particles grown by this method were spheres with diameters of approximately 1 micron. Some larger spheres were also obtained with diameters of up to 25 microns. The CdS spheres were filtered and washed with distilled water. Samples were prepared by suspending the particles in a 5% solution of PMMA in chlorobenzene and spin coated onto fused silica substrates. The particle density was kept low enough so that individual particles were well separated from each other. A photograph of a typical 8 micron diameter CdS sphere obtained using an optical microscope with camera attachment is shown in Figure 3. Since the particles were held rigidly in the PMMA matrix, individual particles could be interrogated by translating the substrate with respect to the focused beam.

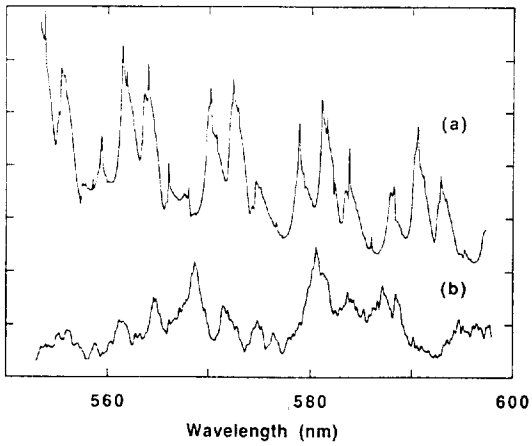

Figure 4. (a) shows the calculated elastic scattering spectrum of a hypothetical 5 μm radius particle of refractive index 2.51 within a medium of index 1.45. (b) shows an experimental scattering curve from a single isolated 6.8 micron radius CdS sphere embedded in PMMA film. Both theoretical and experimental curves display a series of major peaks spaced approximately 2.5 nm apart. In the theoretical case shown in (a), internal scattering was not incorporated within the model and these low order modes maintain exceptionally high Q values ($>10^6$) that are too spectrally narrow to be observed in our limited resolution (1000 point) calculation.

Elastic light scattering measurement used a synchronously pumped, tunable dye laser, that was excited by the second harmonic (532 nm) of a Q-switched and modelocked Nd : YAG laser operating at 1 kHz. The output of the dye laser consisted of pulse trains with Gaussian shaped envelopes containing 20 pulses, each separated from the next by 10 nsec and having a pulse width of approximately 100 psec. The average power was 2 mW at the peak of the dye gain curve. The laser was focused onto individual particles using f/20 optics. Elastically scattered light was collected either at an angle of 30- or 90 -degrees from the forward direction and detected with a photomultiplier tube. A multichanel gated integrator was used for signal averaging.

Results and Discussion

Elastic Light Scattering Measurements. A typical elastic scattering spectrum for a single isolated CdS sphere is shown in Figure 4(b). The spectrum was obtained by scanning the dye laser over the range 553 to 598 nm. Figure 4(a) shows a calculated elastic scattering spectrum of an ideal particle (*i.e.* no absorption nor scattering) with similar morphology ($a=5$ μm, $m=1.731$) for comparison. No attempt was made to exactly match the experimental and theoretical spectra because of the large dispersion in the CdS index of

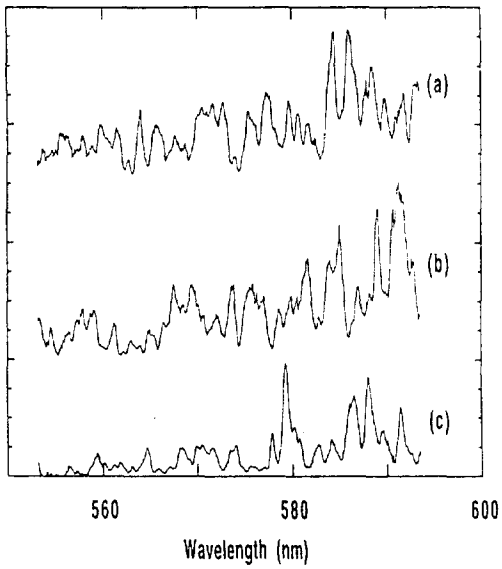

Figure 5. Typical polarized elastic scattering spectra for a single isolated *ca.* 10 micron radius CdS particle embedded in PMMA are shown. Scattering is in the horizonal plane at approximately 90° with respect to the *k* vector of the incident light. In (a), both incident and scattered light are horizontally polarized, yielding a spectrum reflecting the behavior of primarily TM modes. In (b), both input and scattered light are vertically polarized and reflect the scattering of TE modes. In (c) the incident light was vertically polarized and the scattered light was horizontally polarized, reflecting the coupling between TE and TM modes due to crystallite scattering and birefringence. Had the particle been a homogeneous sphere, no depolarized scattering would have been evident. Note that several large peaks in the depolarized spectrum occur at wavelengths corresponding to simultaneous resonance of both TE and TM modes.

refraction[8] in this spectral range (0.1 decrease between 550 and 610 nm) as well as the uncertainty in the magnitude of the internal scattering coefficient resulting from the polycrystalline nature of the sphere. Nevertheless, there are significant similarities between the two curves which make such a comparison useful. Most importantly, the presence of characteristic cavity resonance peaks predicted by theory are confirmed in the experimental spectrum. Note the series of major peaks spaced approximately 2.5 nm apart in both the theoretical and experimental spectra. These are due to modes of one particular order that have *Q*'s in the range 500 to 1000, a value most easily detected with our 0.3 nm experimental spectral resolution. The positions of these features do not change as the incident laser intensity is varied over two orders of magnitude above that used to acquire Figure 4(b). The radius of the particle was estimated to be 6.8 microns based on the wavelength separation, $\Delta\lambda_r$, between successive major peaks using the well-known asymptotic relation[15]: $\Delta\lambda_r/\lambda_r^2 \approx \arctan\,[(m^2-1)^{1/2}]/2\pi a(m^2-1)^{1/2}$. This value was confirmed using optical microscopy (estimated to be 7± 1 μm). Note that the signal-to-noise of Figure 4(b) is much better than the smallest fearures shown and all the fine structure that is visible represents real and reproducible features. This was confirmed by exactly reproducing the spectrum of Figure 4(b) during a series of spectral scans including one taken several days after the first. The sharpest features in this spectrum are a series of low amplitude peaks resembling fine ripple structure superimposed on the major peaks and are especially obvious in the 580 to 660 nm region. A direct measure of their spectral widths leads to a *Q* estimate of about 2000. However, this is a lower limit estimate reflecting the spectral resolution of our probe dye laser and detection system while the actural *Q*'s are much higher as we now show.

Using an approach outlined in Reference 16, which correlates the relative peak heights with known absorption, specifically the self absorption of CdS, we have estimated that the *Q*'s are *ca.* 4×10^4 near 600 nm. We define a Q_β given by[17] $Q_\beta = 2\pi m/\lambda\beta$, where β is the scattering coefficient in cm^{-1} as well as an absorptive cavity quality factor, Q_α, given by[16] $Q_\alpha = 2\pi m/\lambda\alpha$, where α is the absorption coefficient of bulk crystalline CdS in cm^{-1}. The total particle *Q* is given by $1/Q = 1/Q_0 + 1/Q_\alpha + 1/Q_\beta$. Here, Q_0 is determined from Mie theory and represents the ideal non-absorbing homogeneous sphere value which varies greatly with mode number and order. In the CdS polycrystalline particles considered here, except for very low *Q* high order modes, the total *Q* is generally given by $1/Q \approx 1/Q_\alpha + 1/Q_\beta$ (*i.e.* scattering and absorption dominate). When light is in a resonance mode, there is a natural competition between the rate that is absorbed (proportional to $1/Q_\alpha$) and the rate it is coupled out of the particle (proportional to $1/Q_\beta$). When $Q_\alpha \ll Q_\beta$, the mode couples light out too inefficiently to compete with absorption and the mode is not visible in the elastic scattering spectrum. This can be seen by substitution of Q_α and Q_β into an expression for the mode visibility, Φ, given by[17] : $\Phi \approx Q_\alpha/(Q_\alpha+Q_\beta)$. However, when $Q_\alpha \gg Q_\beta$, the scattering coupling dominates and the mode is visible. Examining Figure 4(b) we see that in the region 580 to 600 nm there are a great number of the sharp "ripple" peaks than in the range 560 to 580 nm. We assume that CdS absorption, which increases monotonically as the wavelength decreases[8] in this spectral region, accounts for the difference. Indeed the data appears consistent with $\alpha \approx \beta$ at 580 nm, where the highest *Q* modes start to become less visible at shorter wavelengths and more obvious at higher wavelengths. Using the published value[8] of 4 cm^{-1} at 580 nm and the general expression for Q_β, we estimate that *Q* is as high as *ca.* 4×10^4 in these particles and ultimately limited by the strong internal scattering β value (≈ 4 cm^{-1}). The estimated *Q* value is consistent with the peak heights observed in the 580 nm to 600 nm region since our limited experimental resolution (equivalent to a Q_{exp} of 2000) would reduce the apparent peak heights of such high *Q* modes by about a factor of twenty (*i.e.* the ratio of Q_{exp}/Q) below those of the major peaks.

Figure 5 shows several polarized and depolarized elastic scattering spectra taken of the same 10 micron radius particle. Scattering was viewed in the horizontal plane at an angle of 90 degrees with respect to the *k* vector of the probe light. Figure 5(a) shows data obtained using polarizers to insure that both incident and scattered light were horizontally polarized. The resulting elastic scattering spectrum principally show TM mode features. In Figure 5(b), both incident and scattered light were vertically polarized and TE modes dominate. It can be seen that the spectral positions of the TE and TM resonances usually differ. Because of the high deg-

ree of internal scattering (mechanism depicted in Figure 2 (d)) the actual Q values and output coupling are dominated by this process for wavelength longer than about 570 nm. This leads to the conclusion that the amplitude of the observed elastic scattering in this wavelength regime is directly proportional to the intensity of light just below the surface of particle. In effect, resonance light scattering becomes a probe of the local electric field effect and the peaks seen in Figures 4 and 5 reflect the significant enhancement that occurs at resonances. Figure 5(c) shows the horizontally polarized scattering spectrum obtained using vertically polarized excitation. For the case of an ideal homogeneous sphere, theory[6] predicts that the depolarized scattering at 90 degree is zero. Therefore, the spectrum of Figure 5(c) reflects the deviation of the particle from homogeneity due to birefringence and internal scattering. The large peaks appear to occur in spectral regions where the resonance positions of TE and TM modes coincide and most likely reflect the coupling from TM to TE modes through birefringent polarization rotation.

Photothermal Modulation of Mie Scattering. The presence of significant particle absorption should lead to strong photothermal effects, especially when the photon energy of the excitation source exceeds the bandgap. The absorption cross section for CdS is very large and the quantum yield is small ($<10^3$). As a result, a large fraction of the absorbed light is deposited as heat within the particle. In an effort to determine if heating degrades the cavity behavior of the crystals, a simple photothermal modulation of Mie scattering[18] experiment was performed. Elastically scattered light at 632.8 nm was monitored while the particle was simultaneously illuminated with a 488 nm argon ion laser. The elastic scattering was found to vary by over a factor of two and in an irregular manner in time. The variation of the signal suggested that the effective size parameter (proportional to m and a) for the particle was varing. This is consistent with photothermally induced size expansion and index reduction behavior. Next, the argon ion laser beam was chopped using a variable speed wheel. The response time constant of laser induced changes was found to be approximately 0.5 msec, consistent with the expected thermal response time. Finally, a 500 to 700 nm luminescence curve was obtained using the 488 nm cw excitation. This showed no evidence of MDR features indicating that high Q cavity function was lost under these excitation conditions. Photothermally induced index of refraction inhomogeneities resulting from the front and exit equator lens hot spots and concomitant material expansion bulges near these regions would be expected to degrade the cavity performance. Therefore, under strong photothermal heating, the large cavity resonance enhancement will be lost. This suggests that future studies of microcavity effects in CdS should utilize low level light probes in regions of strong absorption. Note that the nonresonance "lensing" enhancement factor of 8 to 20 (depending on effective m) is relatively unaffected by photothermal effects and would still be present even under strong illumination.

Microcavity Phenomena. As previous authors[2~5] have noted, the presence of a spherical microcavity leads to enhanced local surface fields. This in turn leads to an enhancement in the *amplitude* of the spontaneous emission and Raman scattering signals from surface molecules.[2~4] The spectral changes that also occur in luminescence[19] and spontaneous Raman scattering[20] in spheres are not directly due to this local field effect but result instead from changes in the final density of photon states per unit volume and frequency associated with the presence of a microcavity[10]. In the case of a spherical geometry, this leads to emission rates being enhanced by a factor[13] $9\ m^2D^{3/2}Q/2\pi^3$ on resonance and inhibited by significant factors off resonance. Here D is the mode degeneracy and is equal to $2n+1$. The anticipated enhancement of a 10 micron diameter particle with a Q of 4×10^4 is approximately 1000. This form of enhancement (often called cavity quantum electrodynamic (QED)) involves not only amplitude changes but changes in fundamental molecular parameters (*e.g.* stimulated gain, spontaneous emission lifetimes, etc). Recently, a cavity QED enhancement[13] in excess of 100 was measured in a 14 micron diameter droplet with a quality factor of only 3000, comparable to Q's we observe here. By altering emission rates, cavity QED could, in principle, also modify photochemical rates and pathways. However, this possibility has not been seriously addressed in the literature and so remains an open question. Nevertheless, the presence of both the local field effect and the expected absorption cross section enhancement on resonance, we believe, must certainly affect the photochemistry of CdS, especially below the bandgap (*i.e.* weak absorption region). For example, on resonance, the effective absorption cross section is increased by the ratio, $Q\lambda/4\pi^2am$. Therefore, the resonant absorption cross section of a molecule adsorbed on a micron sized CdS particle will be increased significantly (40 to 1000 times) and the local field strength enhanced 8 to 100 times, yielding a total absorption improvement of 300 to 100,000 times. Note that even in the case of off-resonance or broad-band excitation, the local field effect must necessarily increase the photochemical rates by at least an order of magnitude.

Conclusion

Polycrystalline CdS spheres grown from aqueous solution and embedded in PMMA were studied using elastic light scattering. The presence of sharp peaks in the scattering spectrum confirmed that each microsphere acts as high $Q(>10^4)$ optical cavity, leading to a significant local field effect; *i.e.*, optical fields near the crystal surface are enhanced many times that of the incident radiation's intensity ($<100\times$). A strong depolarized signal confirmed that scattering from internal defects within the crystal provided the main light output coupling mechanism for the cavity, leading to the conclusion that the elastic scattering is proportional to the magnitude of the local field effect. The presence of a greatly enhanced local field effect due to particle lensing and cavity resonances is expected to modify the photophysics of surface adsorbed species, to increase absorption and to affect photochemistry.

Acknowledgment. This work was partially supported by the U.S. Office of Naval Research. S. K. Kim acknowledges the support of a joint NRC/NRL Cooperative Research Fellowship.

References

1. Matijevic, E.; Wilhelmy, D. M. *J. Colloid and Interface*

Sci. **1982**, *86*, 476.
2. Messinger, B. J.; von Raben, K. U.; Chang, R. K.; Barber, P. W. *Phys. Rev. B.* **1981**, *24*, 649.
3. Change, R. K.; Furtak, T. E., eds. *Surface Enhanced Raman Scattering;* Plenum Press: New York, 1982.
4. Hayashi, S.; Koh, R.; Ichuyama, Y.; Yamamoto, K. *Phys. Rev. Lett.* **1988**, *60*, 1085.
5. Wang, Y. *J. Phys. Chem.* **1991**, *95*, 1119.
6. Kerker, M. *The Scattering of Light and Other Electromagnetic Radiation*; Academic Press: New York, 1969.
7. Wiscombe, W. J. *Document PB 301388;* National Technical Information Service: Springfield, VA. 1979.
8. Madelung, O., Ed., *Landolt-Bornstein, New Series, Vol. 17 b*; Springer Verlag: New York, 1983.
9. Benincasa, D. S.; Barber, P. W.; Zhang, J.-Z.; Hsieh, W.-F.; Chang, R. K. *Appl. Opt.* **1987**, *26*, 1348.
10. Ching, S. C.; Lai, H. M.; Young, K. *J. Opt. Soc. Am. B*, **1987**, *4*, 1995; **1987**, *4*, 2004.
11. Hill, S. C.; Benner, R. E. *J. Opt. Soc. Am. B* **1986**, *3*, 1509.
12. Tzeng, H.-M.; Wall, K. F.; Long, M. B.; Chang, R. K. *Opt. Lett.* **1984**, *9*, 499.
13. Campillo, A. J.; Eversole, J. D.; Lin, H.-B. *Phys. Rev. Lett.* **1991**, *67*, 437.
14. Lam, C. C.; Leung, P. T.; Young, K. *J. Opt. Soc. Am. B*, **1992**, *9*, 1585.
15. Chylek, P. *J. Opt. Soc. Am.* **1976**, *66*, 285.
16. Chylek, P.; Lin, H.-B.; Eversole, J. D.; Campillo, A. J. *Opt. Lett.* **1991**, *16*, 1723.
17. Lin, H.-B.; Huston, A. L.; Eversole, J. D.; Campillo, A. J.; Chylek, P. *Opt. Lett.* **1992**, *17*, 970.
18. Lin, H.-B.; Campillo, A. J. *Appl. Opt.* **1985**, *24*, 422.
19. Benner, R. E.; Barber, P. W.; Owen, J. F.; Chang, R. K. *Phys. Rev. Lett.* **1980**, *44*, 475.
20. Thurn, R.; Kiefer, W. *Appl. Opt.* **1985**, *24*, 1515.

Scattering of Noble Gas Ions from a Si(100) Surface at Hyperthermal Energies (20-300 eV)

Hyun-Woo Lee and H. Kang*

Department of Chemistry, Pohang University of Science and Technology, Pohang, Gyeong-buk 790-784, Korea
Received September 1, 1994

In an attempt to understand the nature of hyperthermal ion-surface collisions, noble gas ion beams (He^+, Ne^+, Ar^+, and Xe^+) are scattered from a Si(100) surface for collision energies of 20-300 eV and for 45° incidence angle. The scattered ions are mass-analyzed using a quadrupole mass spectrometer and their kinetic energy is measured in a time-of-flight mode. The scattering event for He^+ and Ne^+ can be approximated as a sequence of quasi-binary collisions with individual Si atoms for high collision energies (E_i>100 eV), but it becomes of a many-body nature for lower energies, Ar^+ and Xe^+ ions undergo multiple large impact parameter collisions with the surface atoms. The effective mass of a surface that these heavy ions experience during the collision increases drastically for low beam energies.

Introduction

Knowledge of the nature of gas-surface collision is important for the processes of adsorption, film deposition, etching, and chemical reactions. Gas-surface scattering technique has been extensively employed for last 20 years in order to obtain information about the collisional nature.[1,2] While these investigations have made significant advances for our understanding of gas-surface collisions, one also becomes realized of a diverse nature of this subject and we are only at the biginning stage of exploration. Depending on collision energy, the nature of scattering can vary from thermal (<1 eV) to binary events (keV). The terminology "hyperthermal" refers to the energy range in which transition between the two different regimes occurs.

Recently, several research groups have explored hyperthermal gas-surface scattering using supersonic atomic beams[3,4] and ion beams.[5~10] In most of these works the mass of a projectile is smaller than a surface atom. The studies of heavy projectile-surface collision is very rare.[3,10] With supersonic beams the collisional energy that can be investigated is limited usually below 10 eV. While ion beams can access to a higher energy, ion scattering has not been widely employed because hyperthermal ion beams are instrumentally difficult to handle and these ions become efficiently neutralized upon surface collisions. In the present work, we have examined the scattering behavior of noble gas ions from a Si surface over a substantially wide range of projectile mass (He^+, Ne^+, Ar^+, and Xe^+) and collision energy (20-300 eV). Such a study enables us to explore the effects of projectile mass and energy on the scattering nature. We find from this study that the heavier ions (Ar^+ and Xe^+) scatter from

*To whom correspondence should be addressed.
This paper is dedicated to Professor Woon-Sun Ahn in honor of his retirement.